

# Global Surface Warming Caused by Shorter-term Radiative Forcings of Aerosols and Ozone in the Last Two Decades

Qing-Bin Lu <sup>1,\*</sup>

Department of Physics and Astronomy, Department of Biology and Department of Chemistry,  
University of Waterloo, 200 University Avenue West, Waterloo, Ontario, Canada

\*Correspondence: qblu@uwaterloo.ca

**Abstract:** Conventional climate models have predicted continuous warming on the Earth's surface and cooling in the upper stratosphere. Here we report observations of regional and global upper stratosphere temperature (UST) and surface temperature and of various climate drivers including greenhouse gases (GHGs), ozone, aerosols, solar variability, snow cover extent, and sea ice extent (SIE), combined with calculations of global mean surface temperature (GMST) by a conceptual physics model. We strikingly found warming trends of  $0.8(\pm 0.6)$  and  $0.7(\pm 0.2)$  K/decade in UST at altitudes of 35-40 km in the Arctic and Antarctic respectively and no significant trends over non-polar regions since 2002. According to the well-recognized climate models, these UST trends provide fingerprints of decreasing (no significant trends) in total GHG effect in polar (non-polar) regions. Correspondingly, we made the first observation of both surface cooling trends in the Antarctic since 2002 and the Arctic since 2016 once the SIE started to recover. But surface warming remains at mid-latitudes, which caused the recent rise in GMST. The latter is quantitatively explained by the positive short-term radiative forcings of aerosols and ozone due to improved air quality. The observed GMST changes agree well with calculated results by the physics model based on halogen-containing GHGs, whose destruction is consistent with the characteristics of the cosmic-ray-driven reaction mechanism with larger rates at higher latitudes. With observations of rapidly lowered aerosol loading, projected halogenated GHGs and stopped Arctic amplification, we predict to observe an emerging long-term GMST reversal that started at the end of 2023.

**Keywords:** physics of climate models; cosmic rays; aerosols; ozone; chlorofluorocarbons (CFCs); Arctic amplification; global warming; global cooling

## 1. Introduction

Some climate models concluded that we must reduce carbon emissions to zero by 2050 to avoid more than 1.5 °C warming [1]. Other than CO<sub>2</sub>, there are certainly other well-mixed greenhouse gases (WMGHGs), e.g., halogen-containing gases (shortened as halo-GHGs hereafter), and short-term radiatively active agents such as aerosols and ozone that are altered due to air pollution [2]. The modeled radiative forcing of CO<sub>2</sub> exhibits a continuously positive trend (see Figure 1a), whereas that of halo-GHGs has shown a plateau since around 2000 due to the regulations by the Montreal Protocol and its Amendments (Figure 1b). Satellite- and ground-based data indicate that aerosol loadings exhibit predominantly negative trends since 2000 over Northern Hemisphere (NH) mid-latitudes and Southern Hemisphere (SH) continents, while increasing over South America (and South Asia and East Africa as well) (Figure 1c). These lead to a globally decreasing aerosol abundance, as assessed in the IPCC AR6 [3]. The AR6 also states that tropospheric ozone increased by 30–70% across the NH from the mid-20th century to the mid-1990s, and that since then, free tropospheric ozone has increased by 2–7% per decade in most regions of NH mid-latitudes, 2–12% per decade in the sampled regions of the NH and SH tropics, and less than 5% per decade at SH mid-latitudes. Simulations by some climate models argued that the shorter-term radiative forcings likely cancel out, and warming is pretty much controlled by just CO<sub>2</sub> emissions (see, e.g., the IPCC Special Report on 1.5 °C warming [1]). This notion implies that surface warming stops when CO<sub>2</sub> emissions stop, i.e., that there is no lag in surface warming once CO<sub>2</sub> emissions reach zero. This is the basis of the concept of the so-called “carbon budget”. However, simulated results by ‘state-of-the-art’ climate models in the IPCC AR6 [3] show that although these short-term effective radiative forcings (ERFs) essentially canceled out during the period 1970-2010, they have led to a positive net forcing of 0.4-0.5 W/m<sup>2</sup> from around 2010 up to the present (Figure 1d). This gives rise to complexities in surface temperature change in the regions (e.g., mid-latitudes) that are experiencing drastic changes in level of air pollution, adding to the greenhouse effect of WMGHGs. For example, Wang et al. [4] investigated regional mean changes in surface air temperatures due to changes in GHGs, aerosol emissions and tropospheric O<sub>3</sub> levels and showed that in 2050 under a carbon neutrality pathway, warming caused by aerosol reductions would dominate climate change over the (sub)regions with surface air temperatures increasing by 0.5–1.4 °C, much higher than the GHG-caused surface temperature increases of below 0.2 °C and the tropospheric O<sub>3</sub> caused surface temperature decreases of less than 0.2 °C. Although the uncertainties in simulated ERFs of aerosols and ozone were assessed as the largest contributors to the overall ERF uncertainty since 1750 in the IPCC AR6 [3], these ERFs should have been better constrained by direct observations of aerosol loadings and tropospheric O<sub>3</sub> since the mid-1990s. Moreover, there are pollution-free regions without such complexities, particularly the Antarctic that has had nearly zero air pollution since 1750 and the Arctic that had eliminated the pollution by around 2000 (Figure 1c).

Additionally, there exist other climate drivers such as solar constant and surface albedo, as well as El Niño and Southern Oscillation (ENSO). ENSO is the most prominent year-to-year climate

fluctuation on Earth, exerting its global impacts through atmospheric teleconnections, affecting extreme weather events worldwide [5, 6]. The total solar irradiance (TSI) had a rising trend from 1700 to 1950, but it has shown a slightly declining trend since 1950, as shown in Figure 2a. Thus, solar constant variability has played a negligible role in surface warming since 1950 [3, 7-10]. Surface albedo is mainly affected by sea-ice extent (SIE) and snow-cover extent (SCE). There was a well-known ‘Arctic amplification’ (AA) effect in surface warming in the Arctic[11], for which Dai et al. [12] proposed a compelling mechanism: it is due to the surface albedo feedback associated with sea-ice loss, leading to increased outgoing longwave radiation and heat fluxes from newly opened waters. This AA mechanism has been overwhelmingly confirmed by our recent observations [13, 14]. Observed data have shown that SCE in NH or North America has stabilized or shown a slight increasing trend since the mid-1990s [13] (Figure 2b), and that SIE in NH largely decreased in 1995-2015 and since 2016, has had an increasing trend, which has not been reported in previous studies [3, 13], given by a polynomial fit to the observed data with 95% confidence (Figure 2c), while SH SIE had a slightly increasing trend in 1995-2015, suddenly dropped in 2015-2016, and since then it has had no significant trend (Figure 2d). As a result, the surface albedo effect and the associated AA effect on surface warming (especially over the NH), which were drastic during 1970-2015, should have terminated since 2016. Thus, the polar regions are now free of both the incontrovertible large uncertainties in simulated ERFs of aerosols given by current climate models and the complexity caused by the AA effect. Therefore, the polar regions have now become an ideal well-controlled laboratory that can directly observe the climate effects of WMGHGs and ODS-caused ozone depletion, both of which are well monitored [14]. All the potential climate drivers are updated and shown in Figures 1a-d and 2a-d, generally consistent with those presented in the IPCC AR6 [3] and our recent studies [13, 14]. These data provide the basis for understanding climate changes from any climate model.

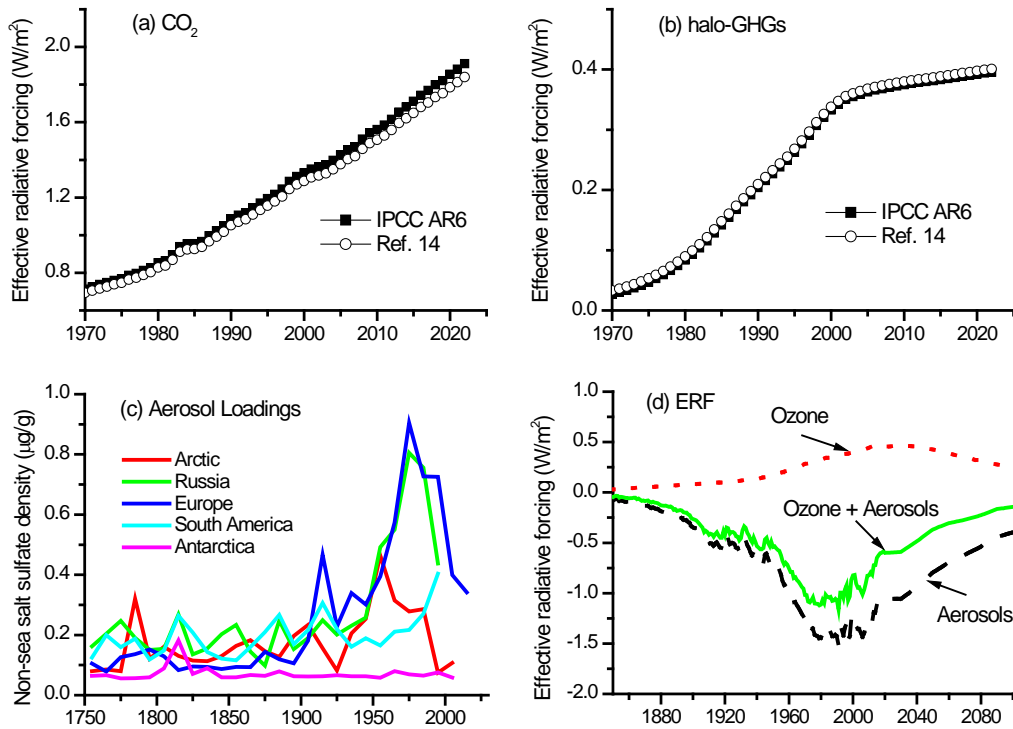


**Figure 1.** (a-b, d) Time-series effective radiative forcings (ERFs) of CO<sub>2</sub>, halo-GHGs, (tropospheric and stratospheric) ozone, aerosols, and the net sum of ozone and aerosols, relative to the pre-industrial period in 1750; (c) 10-year averaged time series of aerosol loadings (concentrations of non-sea salt sulphate) from ice-core measurements. Data are obtained directly from the IPCC AR6 [3], where ERFs were computed by GCMs for the future projection SSP245, or from ERFs calculated in ref. [14].

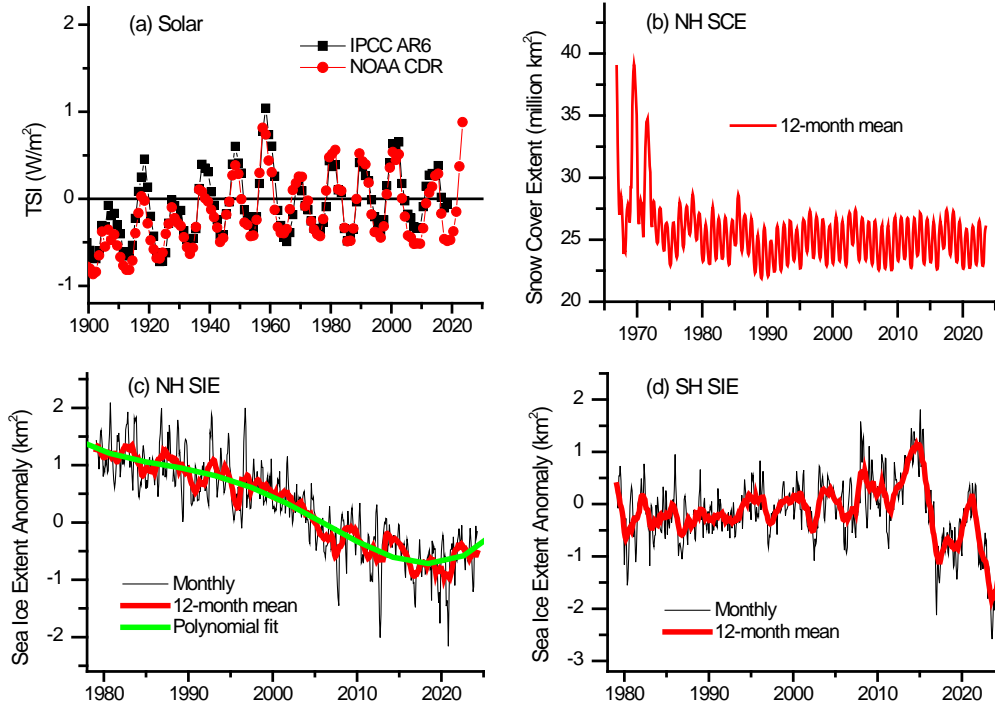


**Figure 2.** (a-d) Time series total solar irradiance (TSI) in 1900-2024, NH snow cover extent (SCE) in 1968-2024, NH and SH sea ice extent (SIE) in 1979-(April) 2024. In (c), a polynomial fit to all the observed NH SIE data with 95% confidence is given (the green line). All data are obtained from the most updated datasets of NOAA, together with the TSI data from IPCC AR6 [3].

Another key observation lies in changes in stratospheric temperature, which reflect changes in surface temperature [15-17]. In conventional climate models, changes in lower stratospheric temperature (LST) are primarily caused by ozone depletion due to emissions of (halogen-containing) ozone-depleting substances (ODSs) [18-20], whereas changes in upper stratospheric temperature (UST) are caused by changing concentrations of WMGHGs (mainly non-halogen GHGs, i.e., CO<sub>2</sub>) and ozone depletion [15, 21]. CO<sub>2</sub>-based climate models have also made an iconic prediction that tropospheric warming and stratospheric cooling would inevitably continue due to the projected continuous increases of CO<sub>2</sub> in the coming decades [3]. Indeed, radiosonde- and satellite-measured data showed that the troposphere warmed and the stratosphere cooled from the mid-1970s to the late 1990s [18-20]. However, most satellite measurements reviewed in the WMO report [18] and the IPCC AR6 [3] showed that the global LST has stabilized since ~1995. It is generally believed that the global LST has dominantly been controlled by ODSs [9, 10, 13, 18, 20, 22, 23]. It is noteworthy that the Manabe-Wetherald climate models [15, 21], recognized by the 2021 Nobel Prize in Physics, have the following important features. Generally, the sensitivity of the surface equilibrium temperature to the change of GHG content such as CO<sub>2</sub> and water vapor is much smaller than that of the stratospheric equilibrium temperature, whereas both

cloudiness and surface albedo have the opposite effect between the sensitivities of surface and stratospheric temperatures. Namely, the sensitivity of the equilibrium UST at 40 km to a change in GHG content is *approximately five times* that of the surface equilibrium temperature. In contrast, the influences of the surface albedo and cloudiness decrease with increasing altitude, having maxima at the earth's surface and being almost negligible at altitudes above 35 km. As a consequence, despite the dependences of temperatures extending from the surface to the lower stratosphere on multiple climate drivers including GHG content, ozone, surface albedo, and cloudiness that introduces the largest uncertainty in radiative forcing given by current climate models [3], *the UST at altitudes above 35 km is predominantly dependent on the GHG content with relatively minor effects from ozone depletion/recovery*. Given this key characteristic, time-series changes in UST if measured properly provide direct fingerprints of the change in total GHG effect. Fortunately, EUMETSAT's ROM SAF satellite data of the troposphere-stratosphere temperature climatology have been available since 2002, providing a source of observational information with high vertical resolution and long-term stability, covering from the troposphere to the upper stratosphere [24-26].

It is well documented in the literature that CO<sub>2</sub>-based climate models (i.e., general circulation models – GCMs) are ‘*quasi-realistic*’, which not only include unresolved terms represented in equations with tunable parameters but also have major limitations such as the structural error and uncertainty across models with different representations of unresolved scales and the requirement of tuning the models to match to observed temperatures [27]. In contrast, the *conceptual* physics model of climate change developed by the author [10], ‘the chlorofluorocarbon (CFC)-warming model’, includes *no tunable parameter* and can give directly *analytical* calculations of variations in GMST caused by halo-GHGs, ozone and solar (aerosol/cloudiness) variability. For a thorough comparison between GCMs and the CFC-warming model, readers are referred to a recent review [14]. This CFC-warming physics model has predicted *a long-term reversal in GMST*, corresponding to the changing trend of atmospheric halo-GHGs[9, 10, 22]. Furthermore, according to the cosmic-ray (CR) driven electron-induced reaction (CRE) mechanism of ODSs for global ozone depletion [9, 10, 22, 23, 28], the destruction of ODSs or halo-GHGs by the CRE reaction is increasingly effective with increasing latitudes due to increasing CR fluxes affected by the geomagnetic field. As a direct consequence, the CFC-warming and CRE models have predicted that the reversal in UST from cooling to warming due to the GHG effect should have occurred first at high latitudes (the polar regions), at which the levels of halo-GHGs (mainly CFCs) decrease first, and will lag by about 10 years over the tropics and mid-latitudes[13, 14]. But this reversal in UST is counteracted by the emerging recovery of the O<sub>3</sub> layer at high latitudes[23], as ozone itself is an effective GHG. Such a counteracting effect should be much smaller at NH than SH high latitudes because O<sub>3</sub> loss over the Arctic is well known to be far less than over the Antarctic since the 1960s. Also, there was a significant increase in tropospheric ozone at NH mid- and high-latitudes due to serious air pollution in the late half of the 20<sup>th</sup> century [3], while tropospheric ozone in the pollution-free Antarctic exhibited little change or some depletion associated with the CRE mechanism [28]. With continuously improving of air quality, it is expected to see a significant

reversal (decrease) in tropospheric ozone at NH mid-latitudes in coming decades [3]. A combination of these effects is expected to see more significant upper-stratospheric warming in the Arctic (and even NH mid-latitudes) than the Antarctic (and even SH mid-latitudes). Correspondingly, a reversal from warming to cooling on the surface should also first occur at high latitudes, which has been observed in the Antarctic[14] and was predicted to emerge in the Arctic once the AA effect on surface temperature becomes insignificant (i.e., the SIE recovers) [13]. These major features of the CFC warming model are generally consistent with observations reported in our recent study [13].

Compared with our earlier studies that used the observed data up to the late 2021/2022 [13, 14], three major advances and/or improvements are made in the current study. (i) We use the updated high-quality EUMETSAT's ROM SAF satellite datasets that have now covered the two complete solar cycles (the past 24 years: 2002-2023) and can therefore provide two 11-year average datasets for the periods 2002-2012 and 2013-2023 to minimize the solar cyclic effect for reliable UST trend analyses. Furthermore, time-series regional UST averaged at altitudes of 35-40 km over the Arctic (60°N-90°N), NH and SH mid-latitudes (30°N-60°N and 30°S-60°S), the tropics (30°S-30°N), and the Antarctic (60°S-90°S) will be presented. Moreover, multiple UST datasets from the EUMETSAT, NOAA, and the UK Met Office will be compared for reliable analyses of UST trends. (ii) More critically, a stabilizing or recovering trend of sea-ice extent, which has not been discovered in earlier studies [3, 13], is now observed for the first time in the monthly NH SIE data up to April 2024 (with an increment of about 20 data points), as shown in Figure 2c. As a result, the stopping of the associated AA effect on surface temperature in the Arctic is now expected to become detectable. (iii) Notably, no short-term radiative forcings of aerosols and ozone were included in our earlier calculations of GMST by the CFC-warming physics model[13, 14], which led to the lower GMSTs than the observed values after 2015. To improve our theoretical calculations of GMSTs, this study will re-calculate GMSTs to include all the ERFs of solar variability, halo-GHGs, aerosols and ozone and their individual contributions to GMST changes will also be identified. With these advances and improvements, this study aims to examine the predictions made by conventional climate models (GCMs) and the CFC-warming model and to precisely reveal the main cause of the GMST rise in the period 2015-2023. The results from this study may lead to the ending of the long-standing debates on the main cause of global warming since the 1970s [9, 10, 22, 29-33].

## **2. Data and Methods**

This study uses the following datasets: The radio occultation data directly provided by the Radio Occultation Meteorology Satellite Application Facility (ROM SAF) which is a decentralized operational RO processing center under EUMETSAT [34, 35]; The data of NOAA surface temperatures v5.1 [36], snow cover extent, sea ice extent, ENSO, total solar irradiance (TSI), and NOAA SSU/AMSU-A upper stratospheric temperatures (Channel 2), obtained directly from the

NOAA; the data of TSI, concentrations of CO<sub>2</sub> and halogenated GHGs, effective radiative forcings of ozone and aerosols were obtained from the IPCC AR6 [3].

To compare with our theoretical GMSTs, the observed GMST data are presented with and without removal of the natural El Niño southern oscillation (ENSO) effect, which is the largest source of year-to-year variability[3, 5]. We simply adopt an empirical approach developed by Lean and Rind [7, 8] to remove the ENSO effect, with details given in previous studies [13, 14].

To calculate GMST changes over the last two decades, we use our CFC-warming physics model with details given previously [10]. Here the CFC model [10, 14] is modified to take into account of the radiative forcings (RFs) of not only halo-GHGs and solar variability but also ozone and aerosols, the GMST change ( $\Delta T_s$ ) becoming

$$\Delta T_s = \lambda_c^{halo} \times (RF^{halo} + RF^{O3}) + \lambda_c^s \times (RF^{solar} + RF^{aerosol}), \quad (1)$$

where  $\lambda_c^s = 0.46 - 0.63 K/(Wm^{-2})$  determined by an observational approach [10, 37] and  $\lambda_c^{halo} = 1.77 K/(Wm^{-2})$  determined from the energy spectrum of the Earth's blackbody radiation given by Planck's formula and the measured atmospheric transmittance spectrum[10]. Like halo-GHGs, ozone has a strong infrared absorption band in the atmospheric window at wavelengths of 8-13  $\mu m$  and therefore the same climate sensitivity to its forcing as halo-GHGs, while aerosols mainly interfere the solar energy reaching Earth's surface and hence share the solar climate sensitivity. RFs of halo-GHGs and solar variability are analytically calculated with a lag of 10 years for halo-GHG forcings [10, 13, 14]. Notably, there is *no tunable parameter* in this conceptual physics model, in strong contrast to GCMs.

### 3. Results and Discussion

Figure 3 shows the results from the ROM SAF datasets for the 11-year mean temperature differences between the last two complete solar cycles (2002-2012 and 2013-2023) to minimize the effect of solar cycles. First, the results in Figures 3a-3b confirm that the entire temperature pattern in the atmosphere closely resembles the atmospheric distribution of CFCs. This observation provides strong visual evidence of the CFC-dominating mechanism of global warming, a conclusion reached in earlier publications [10, 13, 14]. There are clear cooling trends in the polar lower (10-25 km) and tropical middle (25-35 km) stratospheres where ODSs or halo-GHGs are being destructed by the CRE mechanism and the Molina-Rowland photolysis[38] respectively; decreased concentrations of ODSs or halo-GHGs can cause cooling in these atmospheric regions. More importantly, however, it was also clearly demonstrated that cooling in LST was observed to be the most pronounced in polar locations (North Russia and Alaska) where the AA effect



associated with sea-ice melting was large in the 2010s with respect to the 2000s [13]. Second, warming in LST is observed in non-polar regions, as shown in Figures 3a and 3c. This is consistent with previous observations [13, 20] and can be explained by the expected complexes due to multiple climate drivers on LST, including GHG (ODS/halo-GHG) content, ozone depletion/recovery, surface albedo, and cloudiness [15, 21]. Third, most remarkably, the UST at altitudes of 35-40 km has been increased by 0.7 and 1.2 K between the last two solar cycles over the Antarctic and Arctic respectively, and warming trends at altitudes  $\geq 40$  km over non-polar regions are about to emerge (Figures 3a and 3c). This leads to a warming trend in global mean UST (Figure 3c). As stated above and according to the Manabe-Wetherald climate models [15, 21] (see Figure 3d), this warming in UST provides direct evidence that the total greenhouse effect of WMGHGs is decreasing, offering fingerprints of overall decreased GHG content in the globe, particularly in polar (high-latitude) regions. This critical observation is even more pronounced from time-series data of mean UST at altitudes of 35-40 km available for the period 2002-2023 of the Arctic ( $60^{\circ}\text{N}$ - $90^{\circ}\text{N}$ ), NH and SH mid-latitudes ( $30^{\circ}\text{N}$ - $60^{\circ}\text{N}$  and  $30^{\circ}\text{S}$ - $60^{\circ}\text{S}$ ), the tropics ( $30^{\circ}\text{S}$ - $30^{\circ}\text{N}$ ), and the Antarctic ( $60^{\circ}\text{S}$ - $90^{\circ}\text{S}$ ), as shown in Figures 4a-e. Linear fits to the observed data show statistically significant increasing trends in UST of  $0.77(\pm 0.57)$  K/decade and  $0.69(\pm 0.22)$  K/decade in the Arctic and Antarctic respectively and no statistically significant trends in the tropics and mid-latitudes. These results indicate that the total GHG effect has been significantly decreasing in polar regions and has not significantly changed in non-polar regions since the turn of the century. Given the well-measured increasing annual growth rates of atmospheric  $\text{CO}_2$  in the past two decades [3], this observation sharply contradicts the prediction of enhanced cooling trends in UST by  $\text{CO}_2$ -based climate models, but it is in good agreement with the CFC warming model [9, 10, 13, 14, 22] (see Figures 1a-b).

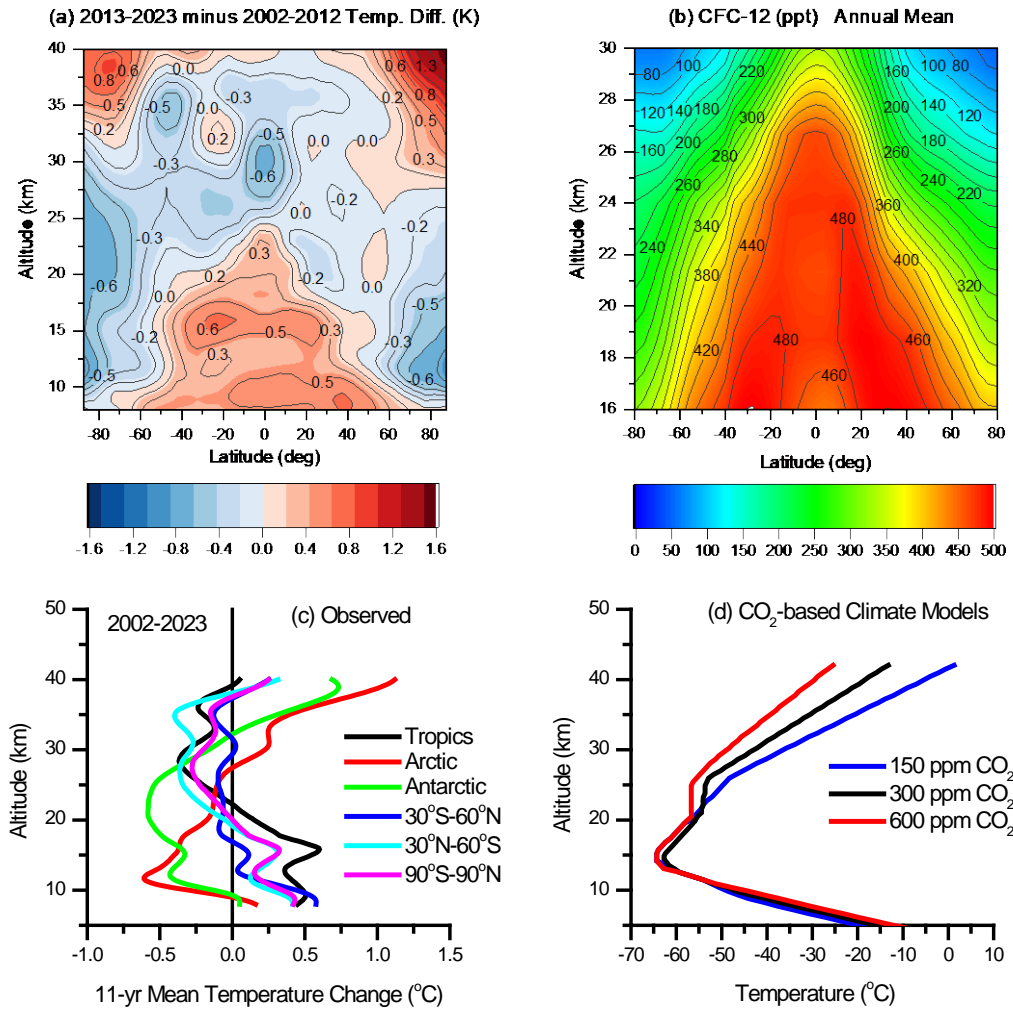


**Figure 3.** Tropospheric-stratospheric temperature (T) climatology, CFC spatial distribution, and CO<sub>2</sub>-climate model prediction. **(a):** T difference in 11-yr mean zonal mean latitude–altitude distribution of the T climatology at altitudes of 8–40 km of 2013-2023 minus 2002-2012, obtained from the EUMETSAT’s ROM SAF satellite datasets. **(b):** Representative zonal mean latitude–altitude distribution of the CF<sub>2</sub>Cl<sub>2</sub> concentration, obtained from the NASA UARS’s CLEAS dataset. **(c):** Observed altitude profiles of the 11-yr mean T difference over the last two solar cycles for the tropics (30° S–30° N), Antarctic (60°–90° S), Arctic (60°–90° N), mid-latitudes (30°–60° S/N) and the globe (90°S–90°N) of the Earth. **(d):** GCM-modeled altitude profiles of the variation in the troposphere and stratosphere T due to increased levels (150 ppm, 300 ppm, and 600 ppm) of atmospheric CO<sub>2</sub>. **(a–c):** Modified and updated from Lu[13, 14]; **(d):** adapted from the Illustration and Popular science background for the 2021 Nobel Prize in Physics by the Royal Swedish Academy of Sciences, which originated from the Manabe-Wetherald climate model [15].

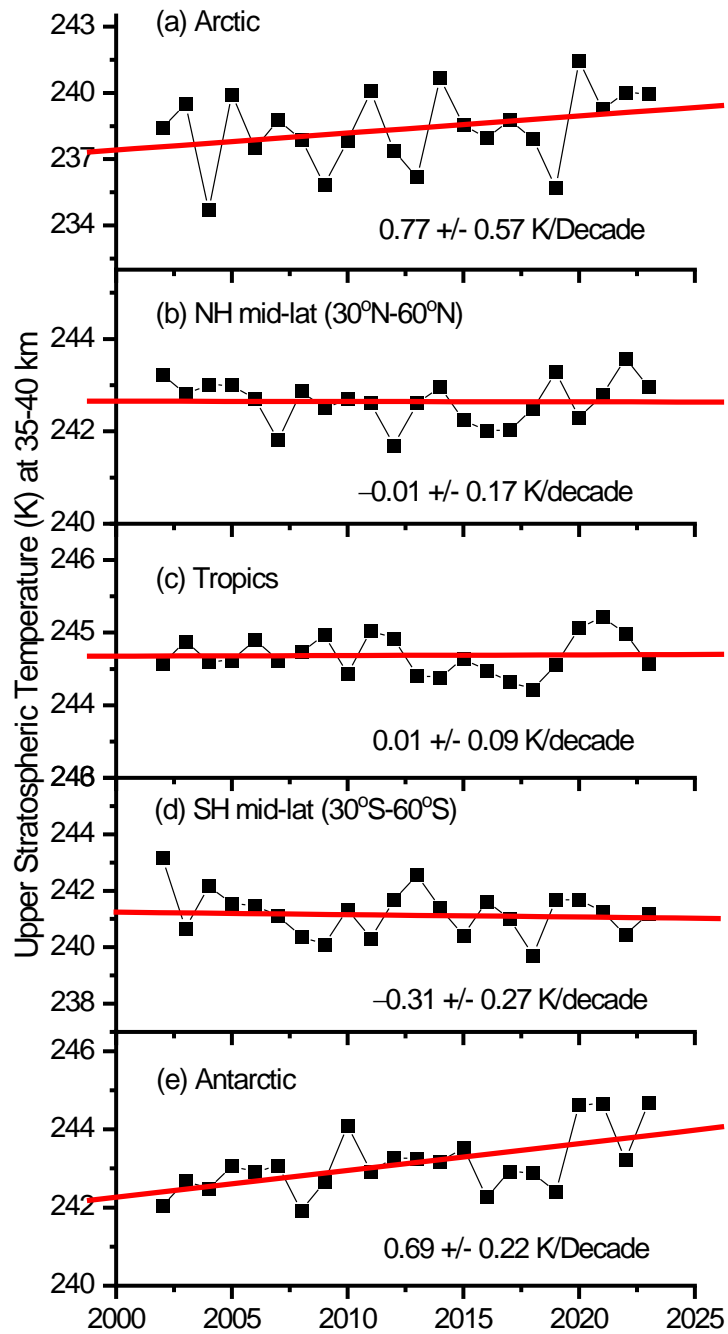


**Figure 4.** (a)-(e): Time-series annual upper stratospheric temperature (UST) averaged at altitudes of 35-40 km, obtained from the EUMETSAT's ROM SAF satellite datasets. The red lines are linear fits to the observed datasets.

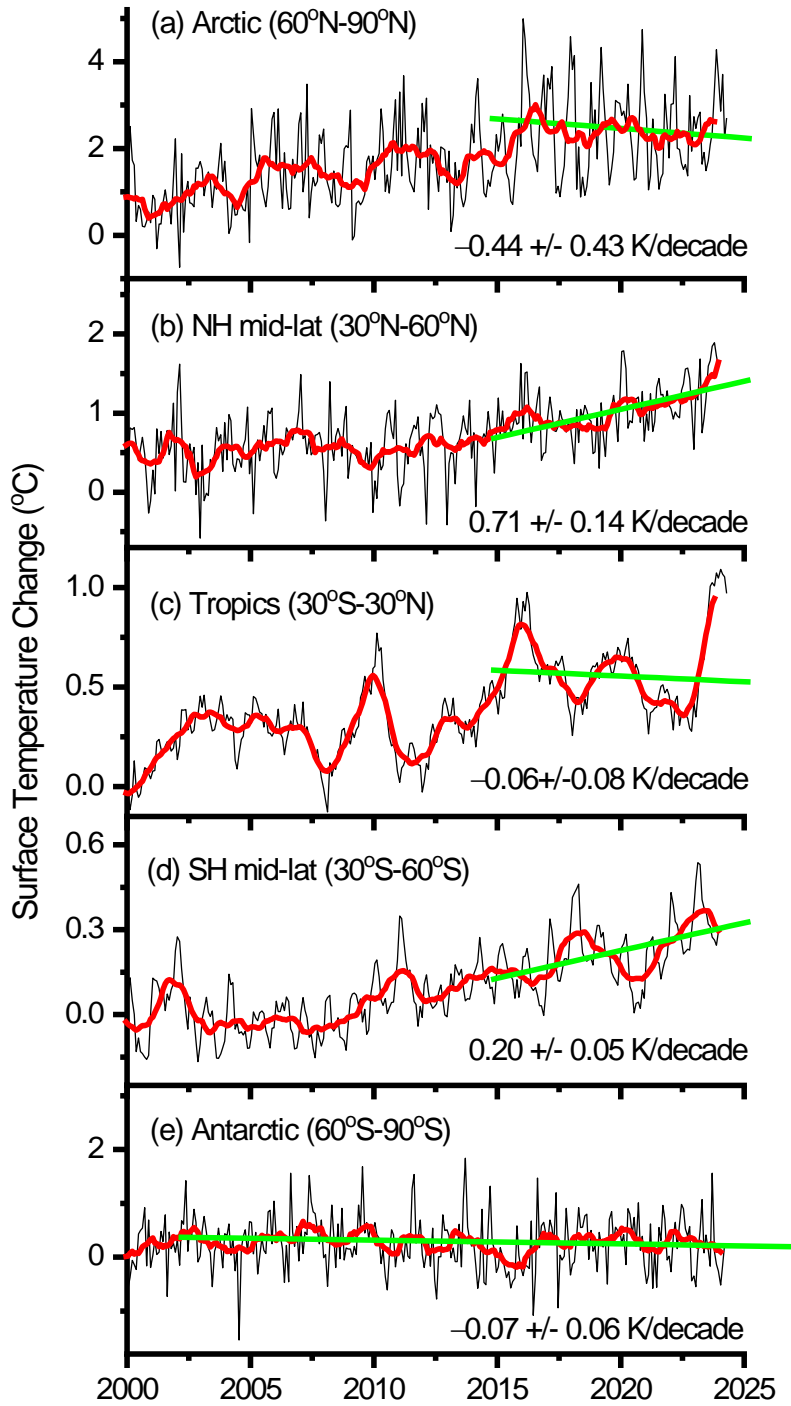


**Figure 5.** (a)-(e): Observed monthly regional surface temperatures obtained from the NOAA 5.1. The red curves are 12-month averaging to the observed datasets; the green lines are linear fits to the observed datasets.

Correspondingly, time-series data of surface temperatures for the period 2000-2023 of the Arctic (60°N-90°N), Northern and Southern mid-latitudes (30°N-60°N and 30°S-60°S), the tropics (30°S-30°N), and the Antarctic (60°S-90°S), obtained from the most updated NOAA5.1 datasets [36], are shown in Figures 5a-e. It is particularly interesting to observe that consistent with the UST trends observed in Figures 4a-e, the surface temperatures exhibit weakly decreasing trends in both the Antarctic since 2002 and the Arctic since 2016 and no statistically significant trend in the tropics. The changes in the Antarctic surface temperature since 1980 stand in contrast to the equilibrium warming pattern simulated by Earth system models (ESMs) under CO<sub>2</sub> radiative forcing even taking into account of ocean dynamics, as acknowledged in the IPCC AR6 (Chapter 7, p. 987) [3]. But they are excellently reproduced by the calculations using the CFC-warming model with inputs of halo-GHGs and ozone depletion alone [14]. Most remarkably, the Arctic surface temperature has a sensitive response to the emerging recovery in NH SIE (Figure 2c), consistent with the well-known dominance of the AA effect prior to 2016 [39]. In contrast, there are still significantly increasing trends in surface temperature at both SH and NH mid-latitudes, which are  $0.20 \pm 0.05$  °C/decade and  $0.71 \pm 0.14$  °C/decade respectively, despite no significantly cooling trends in UST over the regions (Figures 4b and 4d). These warmings in surface temperature, however, are consistent with the observed declining trends in atmospheric aerosol loading in the regions: as shown in Figure 1c, aerosol loadings are rapidly decreasing at mid-latitudes, which have negligible effects on UST at altitudes above 35 km [15, 21] but generate positive radiative forcing (Figure 1d) leading to surface warming there. In addition, there is also a small positive radiative forcing of ozone (Figure 1d). The results in Figures 4 and 5 clearly indicate that surface warming at mid-latitudes, which take up 36.6% in area of the globe, is caused by reduced air pollution and responsible for the rise in GMST in the period 2016-2023.

To obtain a quantitative understanding of the GMST changes over the last two decades, we calculate GMST changes by the CFC-warming physics model with the details given in Data and Methods, in view of the fact that the modeled CO<sub>2</sub> radiative forcing is apparently missing in the observed data shown in Figures 3-5 and previously [9, 10, 13, 14, 22, 29-33]. As shown in Figure 6, our calculated results of GMST exhibit overall good agreement with the observed GMST data in 2000-2023. The observed data are presented both in original form and with removal of the contribution of the natural ENSO [7, 8, 13, 14]. We note that our calculated GMSTs after 2016 are slightly lower than the GMSTs given by Version 5.1 of the NOAA dataset. These small discrepancies, however, are more likely caused artificially by the NOAA data processing than by our CFC-warming model, since historical GMSTs in the period 2000-2012 given in the IPCC AR6 [3] are higher by about 0.09 °C than those given in the IPCC AR5 [19] due to ‘changes in observational understanding’ and we have demonstrated that GMSTs after 2016 in the version of either NOAA 5.1 or UK Met Office’s HadCRUT5 are higher than those in their earlier versions (e.g., HadCRUT4.6 or NOAA 4.0) [14]. The four individual contributions of solar irradiance variability, halo-GHGs, ozone, and aerosols to GMST changes, are plotted in Figures 7a-7d. All the results are relative to their 1995-2005 means. These results clearly show that the rise in GMST

in the past decade is mainly caused by the positive short-term radiative forcings of ozone and aerosols as a result of reduced air pollution, which has occurred in mid-latitude regions, with relatively minor contributions from halo-GHGs and solar variability. This is consistent with the observed results of regional USTs and surface temperatures shown in Figures 4 and 5. With the observations of rapidly lowered aerosol loading, slowly peaking halo-GHGs, and stopped Arctic amplification, we expect to see an emerging reversal in GMST. It is noteworthy that the current net radiative forcing from ozone and aerosols has returned and been close to its global level in the 1950s (Figure 1d). Thus, the effects of aerosols and ozone on GMST in coming decades should be very limited. Moreover, both the TSI peak in the current solar cycle and the ENSO signal peak occurred in October and November 2023 respectively, as seen in observed data, and the responses in GMST to TSI and ENSO variability have short delays of only 1-4 months [7, 8, 13]. Indeed, the observed GMST data, after removal of the ENSO effect through an established approach by Lean and Rind [7, 8], exhibit a peak around October 2023 and since then, has been decreasing over the past six months, in spite of the peaking in the responses of GMST to both TSI and ENSO variabilities. Thus, it seems optimistic to expect a continuous long-term reversal in GMST, which likely already started in the end of 2023 and will exhibit a cooling trend in next 5-10 years (Figure 6).

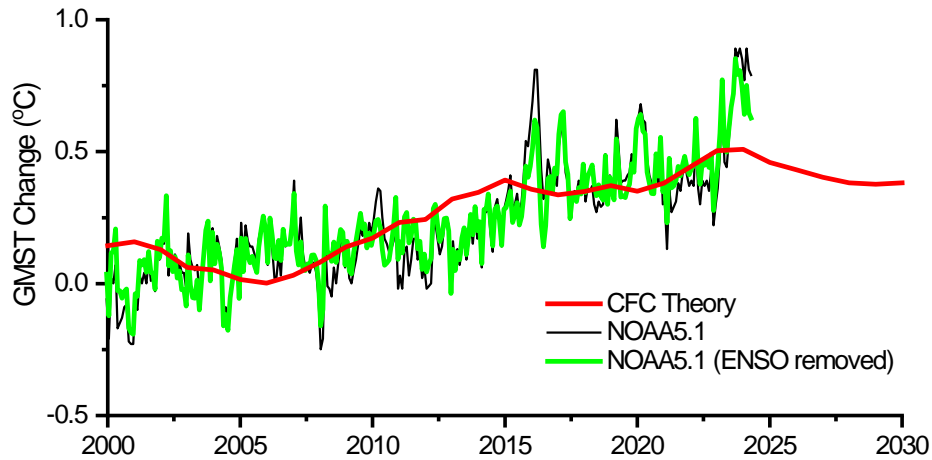


**Figure 6.** Observed and calculated GMSTs. Observed GMST data were the NOAA5.1 combined land surface air temperature and sea surface temperature anomalies (thin black line: original monthly data; thick green line: after removal of the natural ENSO effect). Calculated GMSTs (thick red line) are obtained by the CFC-warming model including the contributions of halo-GHGs, the solar effect, ozone, and aerosols. All the results are relative to their 1995-2005 means.

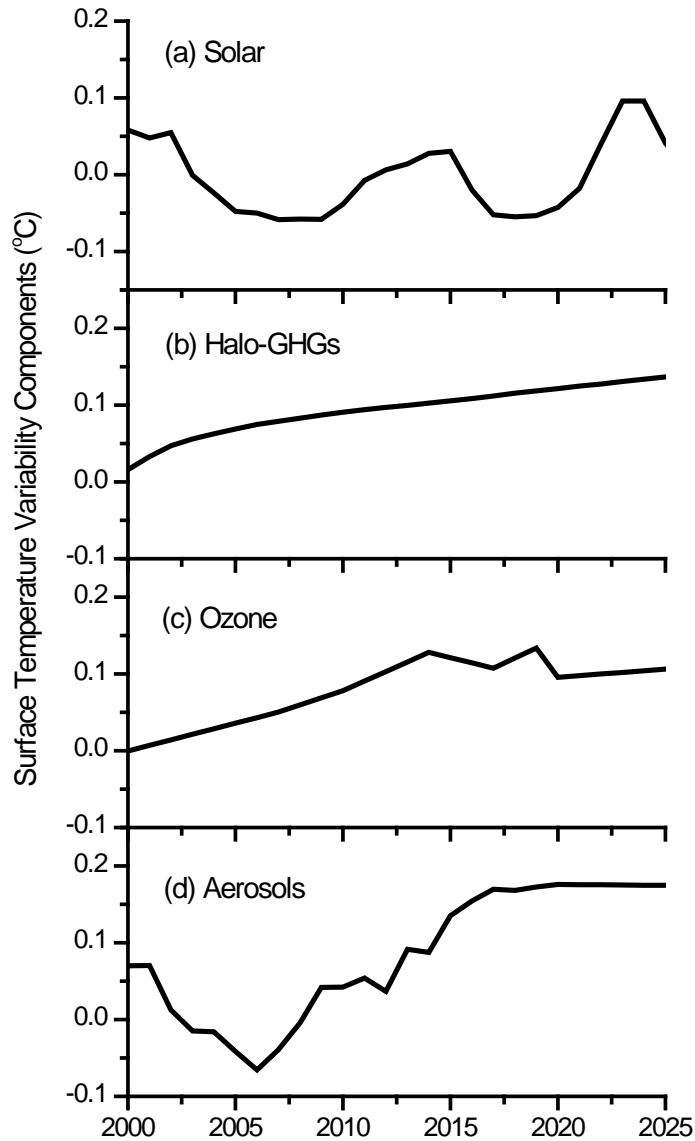


**Figure 7.** Calculated individual contributions of the solar effect, halo-GHGs, ozone, and aerosols to the GMST change by the CFC-warming model. Each of the results is relative to the 1995-2005 mean.

Finally, we must note that our observed UST trends in ROM SAF data displayed in Figures 3 and 4 show different trends from the NOAA STAR reprocessed UST data of Stratospheric Sounding Unit (SSU) and Advanced Microwave Sounding Unit (AMSU)-A (Channels 1-3). The latter provide data on temperatures in the middle and upper stratosphere, but they encounter formidable problems in deriving UST trends, which are subject to calibration issues in the SSU/AMSU space-view anomaly and radiometric anomalies, changing pressures in the pressure modulator cells, solar tides, and atmospheric CO<sub>2</sub> concentration changes in the satellite observations [16, 17, 40, 41]. In

the two independently processed SSU datasets [16, 17, 40, 42], the NOAA STAR data were found to have striking differences in stratospheric temperature trends from those earlier processed by the UK Met Office (UKMO) [43]. For example, the global-mean cooling in SSU channels 1 and 2 sampling the middle stratosphere (around 25–45 km) in the NOAA data set was nearly twice as large as that in the UKMO data set. The differences between the NOAA and UKMO global-mean time series were so large that they called into question the fundamental understanding of observed temperature trends in the middle and upper stratosphere from the SSU data. Since the SSU measured the radiances from emission by atmospheric CO<sub>2</sub>, the weighting functions of its different channels were subject to time-varying changes, which was based on the understanding from CO<sub>2</sub> climate models[40, 42]. Owing to increasing atmospheric CO<sub>2</sub>, the weighting functions of the three SSU channels were modeled to shift to higher altitudes at higher temperatures, and hence spurious positive temperature trends were presumably superimposed on the SSU temperature trends and corrected from the original data in the NOAA STAR dataset [40, 42]. Not surprisingly, such revised trends become significantly more negative (cooling) in the middle and upper stratosphere, though they are expectedly in better agreement with CO<sub>2</sub> model-calculated trends that are expected to be negative throughout the stratosphere. However, the simulated impact of changes in CO<sub>2</sub> on the weighting functions and hence the measured radiances can be seriously problematic, provided with the documented satellite observations showing that the 15- $\mu$ m atmospheric CO<sub>2</sub> absorption band was actually missing in the observed radiance difference spectrum in the rapidly warming period 1970-1999 [10, 14, 44, 45]. The latter observation is in striking contrast to what is expected from CO<sub>2</sub>-based climate models. Although both NOAA and UKMO SSU datasets have been reprocessed and documented and differences between them have been reduced, there remain major discrepancies [41, 46, 47].

As shown in Figure 8, the UKMO reprocessed dataset[41] for SSU2 (at altitudes of 35-45 km) seems consistent with the global mean UST trend at 35-40 km obtained from the ROM SAF data but the NOAA STAR SSU/AMSU-A dataset does not, though the UKMO data are available only as globally 6-month mean data. Slightly differently from the NOAA STAR reprocessing, the UKMO data reprocessing used the computed weighting functions for the SSU channels with a selected temperature anomaly profile to produce a temperature best matching the observed temperature changes in each SSU channel[41]. It is noteworthy that the UKMO reprocessed SSU time series are very close to those analyzed by several independent groups after the recommended corrections for radiometric, spectroscopic and tidal differences to resolve the discrepancies among SSU datasets[41]. The consensus results are the following: a cooling trend over 1979–1996 is seen in all three SSU channels, while a weakly warming trend of  $0.13 \pm 0.1$  K in Channel 2 and no statistically significant cooling trends of  $-0.05 \pm 0.1$  K in Channel 1 and  $-0.12 \pm 0.3$  K in Channel 3 over 1997-2006 are observed[41]. Similarly, Randel et al.[48] found near zero trends in time-series de-seasonalized temperature anomalies for SSU2 at the equator, 50°S, and 80°S during 2000-2015, with data from the NOAA SSU, the Aura Microwave Limb Sounder (MLS) and Sounding of the Atmosphere Using Broadband Emission Radiometry (SABER) instruments. In Figure 8, a linear



fit to the ROM SAF data gives a weakly warming trend of  $0.04 \pm 0.02$  K/decade during 2002-2023, which is very close to the weakly warming trend during 1997-2006 observed by Nash and Saunders[41] and the near zero trend during 2000-2015 observed by Randel et al.[48] Notably, the pronounced UST cooling trends over 2002-2023 in all three SSU channels obtained from the NOAA STAR data (Channels 1 and 3 are not shown) are not consistent with the observed trends in surface temperature (Figure 5), independent of CO<sub>2</sub>-based climate models or the CFC-warming model. It seems very likely that the UST cooling trends derived from the model-corrected NOAA STAR datasets arise from artificial effects caused by the above-mentioned data calibration problems.

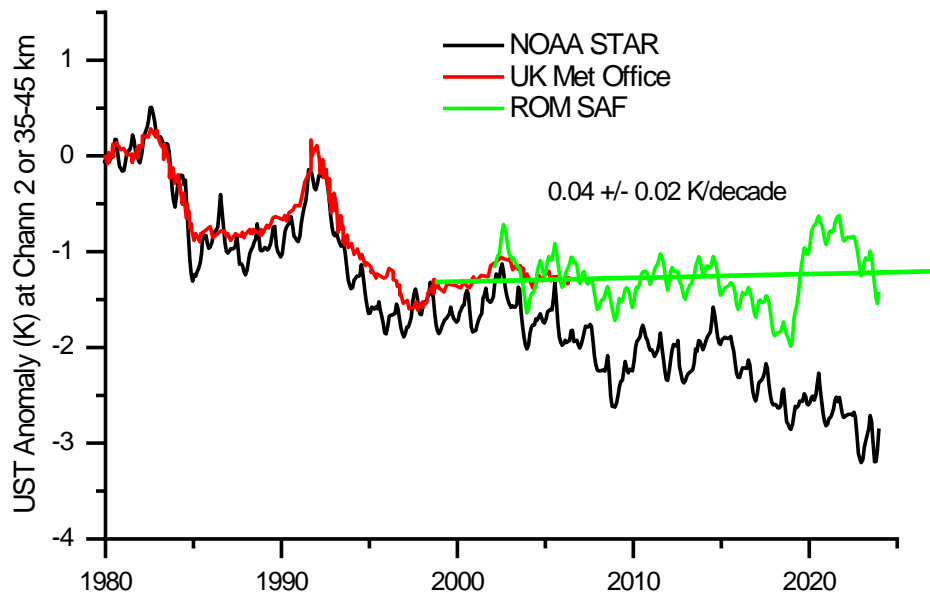


**Figure 8.** Time-series upper stratospheric temperatures (USTs) in 1980-2023, obtained from the EUMETSAT’s ROM SAF satellite dataset at altitudes of 35-40 km, UK Met Office (UKMO) and NOAA STAR SSU/AMSU-A datasets (Channel 2, 35-45 km).

## 7. Conclusion

In contrast to the predicted continuous warming on the surface and cooling in the upper stratosphere by CO<sub>2</sub>-based climate models, a consistent phenomenon observed from both UST and surface temperature measurements on the global scale has emerged. The observed data strikingly show that the UST at altitudes of 35-40 km exhibits warming trends in polar regions and no significant trends in non-polar regions since 2002, and that correspondingly surface temperature exhibits cooling trends in the Antarctic since 2002 and in the Arctic since 2016 when the SIE-

associated AA effect stopped, and no statistically significant trend in the tropics since 2016. In contrast, there remain significant surface warming trends at SH and NH mid-latitudes, which are responsible for the recent rise in GMST in the last two decades. This warming, however, is quantitatively explained by the IPCC-documented positive short-term radiative forcings of aerosols and ozone as a result of improved air quality. According to well-recognized climate models, the observed UST trends provide strong evidence that the total GHG effect has been decreasing in polar regions and not significantly increased in non-polar regions in the last two decades, leading to an overall decreasing trend in global GHG effect. These observations are in quantitative agreement with the calculated results by the parameter-free physics model based on halo-GHGs, whose destruction is consistent with the features of the CRE mechanism. The latter gives larger rates in destruction of halo-GHGs and hence earlier reversals in surface and upper-stratospheric temperatures at higher latitudes (polar regions). With observations of rapidly lowered aerosol loading, projected halo-GHGs, and terminated AA effect, we expect to see an emerging reversal in GMST, which likely started in the end of 2023 and will show a cooling trend in next 5-10 years. Future testing of this prediction will be interesting.

**Funding:** This research was funded by the Natural Science and Engineering Research Council of Canada and the University of Waterloo.

**Data Availability Statement:** The data used for this study were obtained from the following sources: The radio occultation data were provided by the Radio Occultation Meteorology Satellite Application Facility (ROM SAF) which is a decentralized operational RO processing center under EUMETSAT. ROM SAF RO data are available at: <http://www.romsaf.org> [34, 35]. The data of NOAA surface temperatures (v5.1) (<https://www.ncei.noaa.gov/data/noaa-global-surface-temperature/v5.1/access/timeseries/>) [36], snow cover extent and sea ice extent (<https://www.ncei.noaa.gov/access/monitoring/snow-and-ice-extent/>), ENSO (<https://www.cpc.ncep.noaa.gov/data/indices/>), total solar irradiance (TSI) (<https://www.ncei.noaa.gov/products/climate-data-records/total-solar-irradiance>), and NOAA SSU/AMSU-A upper stratospheric temperatures (Channel 2) were obtained from the NOAA (<https://www.star.nesdis.noaa.gov/smcd/emb/mscat/>); the data of TSI, concentrations of CO<sub>2</sub> and halogenated GHGs, effective radiative forcings of ozone and aerosols were obtained from the IPCC AR6 (<https://www.ipcc.ch/report/ar6/wg1/>) [3]; zonal mean latitude–altitude distribution of CF<sub>2</sub>Cl<sub>2</sub> (CFC-12) was obtained from the NASA UARS (CLEAS) dataset (<https://earthdata.nasa.gov/>)[13].

**Acknowledgments:** The author is greatly indebted to the Science Teams for making the data used for this study available. The author also thanks Professor Anthony Leggett for his helpful and constructive comments on an earlier version of this manuscript.

**Conflicts of Interest:** The author declares no conflict of interest.

## References

1. IPCC, *Special Report on Global Warming of 1.5°C*; Cambridge University Press: Cambridge, UK, 2018.
2. P. Chlek, J.A. Coakley, *Aerosols and Climate, Science*, 183 (1974) 75-77.
3. IPCC, *AR6 Climate Change 2021: The Physical Science Basis*; Cambridge University Press: Cambridge, UK, 2023.
4. P. Wang, Y. Yang, D. Xue, L. Ren, J. Tang, L.R. Leung, H. Liao, Aerosols overtake greenhouse gases causing a warmer climate and more weather extremes toward carbon neutrality, *Nat. Comm.*, 14 (2023) 7257.
5. S.-W. Yeh, J.-S. Kug, B. Dewitte, M.-H. Kwon, B.P. Kirtman, F.-F. Jin, El Niño in a changing climate, *Nature*, 461 (2009) 511-514.
6. J.D. Rojo Hernández, Ó.J. Mesa, U. Lall, ENSO Dynamics, Trends, and Prediction Using Machine Learning, *Weather and Forecasting*, 35 (2020) 2061-2081.
7. J.L. Lean, D.H. Rind, How natural and anthropogenic influences alter global and regional surface temperatures: 1889 to 2006, *Geophysical Research Letters*, 35 (2008) L18701.
8. J.L. Lean, D.H. Rind, How will Earth's surface temperature change in future decades?, *Geophysical Research Letters*, 36 (2009) L15708.
9. Q.-B. Lu, Cosmic-ray-driven reaction and greenhouse effect of halogenated molecules: culprits for atmospheric ozone depletion and global climate change, *International Journal of Modern Physics B*, 27 (2013) 1350073.
10. Q.-B. Lu, *New Theories and Predictions on the Ozone Hole and Climate Change; World Scientific: Hackensack, NJ, USA, 2015; pp.141–252.*
11. P. Chylek, C. Folland, J.D. Klett, M. Wang, N. Hengartner, G. Lesins, M.K. Dubey, Annual Mean Arctic Amplification 1970–2020: Observed and Simulated by CMIP6 Climate Models, *Geophysical Research Letters*, 49 (2022) e2022GL099371.
- A. Dai, D. Luo, M. Song, J. Liu, Arctic amplification is caused by sea-ice loss under increasing CO<sub>2</sub>, *Nature Communications*, 10 (2019) 121.
12. Q.-B. Lu, Major Contribution of Halogenated Greenhouse Gases to Global Surface Temperature Change, *Atmosphere*, 13 (2022) 1419.
13. Q.-B. Lu, Critical Review on Radiative Forcing and Climate Models for Global Climate Change since 1970, *Atmosphere*, 14 (2023) 1232.
14. S. Manabe, R.T. Wetherald, Thermal Equilibrium of the Atmosphere with a Given Distribution of Relative Humidity, *Journal of Atmospheric Sciences*, 24 (1967) 241-259.
15. J. Nash, G.F. Forrester, Long-term monitoring of stratospheric temperature trends using radiance measurements obtained by the TIROS-N series of NOAA spacecraft, *Advances in Space Research*, 6 (1986) 37-44.
16. J. Nash, Extension of explicit radiance observations by the Stratospheric Sounding Unit into the lower stratosphere and lower mesosphere, *Quarterly Journal of the Royal Meteorological Society*, 114 (1988) 1153-1171.

17. WMO/UNEP, *Scientific Assessment of Ozone Depletion: 2018*; WMO Global Ozone Research and Monitoring Project—Report No. 58; WMO: Geneva, Switzerland, 2018.
18. IPCC, *AR5 Climate Change 2013: The Physical Science Basis*; Cambridge University Press: Cambridge, UK, 2013.
19. R. Philipona, C. Mears, M. Fujiwara, P. Jeannot, P. Thorne, G. Bodeker, L. Haimberger, M. Hervo, C. Popp, G. Romanens, W. Steinbrecht, R. Stübi, R. Van Malderen, Radiosondes Show That After Decades of Cooling, the Lower Stratosphere Is Now Warming, *Journal of Geophysical Research: Atmospheres*, 123 (2018) 12,509-512,522.
20. S. Manabe, R.T. Wetherald, The Effects of Doubling the CO<sub>2</sub> Concentration on the climate of a General Circulation Model, *Journal of Atmospheric Sciences*, 32 (1975) 3-15.
21. Q.-B. Lu, Cosmic-ray-driven electron-induced reactions of halogenated molecules adsorbed on ice surfaces: Implications for atmospheric ozone depletion and global climate change, *Physics Reports-Review Section of Physics Letters*, 487 (2010) 141-167.
22. Q.-B. Lu, Fingerprints of the cosmic ray driven mechanism of the ozone hole, *AIP Advances*, 11 (2021) 115307.
23. E.R. Kursinski, G.A. Hajj, J.T. Schofield, R.P. Linfield, K.R. Hardy, Observing Earth's atmosphere with radio occultation measurements using the Global Positioning System, *Journal of Geophysical Research: Atmospheres*, 102 (1997) 23429-23465.
24. A.K. Steiner, F. Ladstädter, C.O. Ao, H. Gleisner, S.P. Ho, D. Hunt, T. Schmidt, U. Foelsche, G. Kirchengast, Y.H. Kuo, K.B. Lauritsen, A.J. Mannucci, J.K. Nielsen, W. Schreiner, M. Schwärz, S. Sokolovskiy, S. Syndergaard, J. Wickert, Consistency and structural uncertainty of multi-mission GPS radio occultation records, *Atmos. Meas. Tech.*, 13 (2020) 2547-2575.
25. H. Gleisner, K.B. Lauritsen, J.K. Nielsen, S. Syndergaard, Evaluation of the 15-year ROM SAF monthly mean GPS radio occultation climate data record, *Atmos. Meas. Tech.*, 13 (2020) 3081-3098.
26. V. Balaji, F. Couvreux, J. Deshayes, J. Gautrais, F. Hourdin, C. Rio, Are general circulation models obsolete? *Proceedings of the National Academy of Sciences*, 119 (2022) e2202075119.
27. Q.-B. Lu, Formulation of the cosmic ray-driven electron-induced reaction mechanism for quantitative understanding of global ozone depletion, *Proceedings of the National Academy of Sciences*, 120 (2023) e2303048120.
28. K.Y. Kondratiev, H.I. Niilisk, On the question of carbon dioxide heat radiation in the atmosphere, *Geofisica pura e applicata*, 46 (1960) 216-230.
29. R.E. Newell, T.G. Dopplick, Questions Concerning the Possible Influence of Anthropogenic CO<sub>2</sub> on Atmospheric Temperature, *Journal of Applied Meteorology and Climatology*, 18 (1979) 822-825.
30. S.B. Idso, The Climatological Significance of a Doubling of Earth's Atmospheric Carbon Dioxide Concentration, *Science*, 207 (1980) 1462-1463.
31. R.S. Lindzen, Can increasing carbon dioxide cause climate change?, *Proceedings of the National Academy of Sciences*, 94 (1997) 8335-8342.

32. D.H. Douglass, J.R. Christy, B.D. Pearson, S.F. Singer, A comparison of tropical temperature trends with model predictions, *International Journal of Climatology*, 28 (2008) 1693-1701.
33. H. Gleisner, M.A. Ringer, S.B. Healy, Monitoring global climate change using GNSS radio occultation, *npj Climate and Atmospheric Science*, 5 (2022) 6.
34. F. Ladstädter, A.K. Steiner, H. Gleisner, Resolving the 21st century temperature trends of the upper troposphere–lower stratosphere with satellite observations, *Scientific Reports*, 13 (2023) 1306.
35. R.S. Vose, B. Huang, X. Yin, D. Arndt, D.R. Easterling, J.H. Lawrimore, M.J. Menne, A. Sanchez-Lugo, H.M. Zhang, Implementing Full Spatial Coverage in NOAA’s Global Temperature Analysis, *Geophysical Research Letters*, 48 (2021) e2020GL090873.
36. D.H. Douglass, B.D. Clader, Climate sensitivity of the Earth to solar irradiance, *Geophysical Research Letters*, 29 (2002) 33-31-33-34.
37. M.J. Molina, F.S. Rowland, STRATOSPHERIC SINK FOR CHLOROFLUOROMETHANES - CHLORINE ATOMIC-CATALYSED DESTRUCTION OF OZONE, *Nature*, 249 (1974) 810-812.
- A. Dai, J.C. Fyfe, S.-P. Xie, X. Dai, Decadal modulation of global surface temperature by internal climate variability, *Nature Climate Change*, 5 (2015) 555-559.
38. K.P. Shine, J.J. Barnett, W.J. Randel, Temperature trends derived from Stratospheric Sounding Unit radiances: The effect of increasing CO<sub>2</sub> on the weighting function, *Geophysical Research Letters*, 35 (2008).
39. J. Nash, R. Saunders, A review of Stratospheric Sounding Unit radiance observations for climate trends and reanalyses, *Quarterly Journal of the Royal Meteorological Society*, 141 (2015) 2103-2113.
40. L. Wang, C.-Z. Zou, H. Qian, Construction of Stratospheric Temperature Data Records from Stratospheric Sounding Units, *Journal of Climate*, 25 (2012) 2931-2946.
41. D.W.J. Thompson, D.J. Seidel, W.J. Randel, C.-Z. Zou, A.H. Butler, C. Mears, A. Osso, C. Long, R. Lin, The mystery of recent stratospheric temperature trends, *Nature*, 491 (2012) 692-697.
42. H.E. Brindley, R.P. Allan, Simulations of the effects of interannual and decadal variability on the clear-sky outgoing long-wave radiation spectrum, *Quarterly Journal of the Royal Meteorological Society*, 129 (2003) 2971-2988.
43. J.G. Anderson, J.A. Dykema, R.M. Goody, H. Hu, D.B. Kirk-Davidoff, Absolute, spectrally-resolved, thermal radiance: a benchmark for climate monitoring from space, *Journal of Quantitative Spectroscopy and Radiative Transfer*, 85 (2004) 367-383.
44. C.-Z. Zou, H. Qian, Stratospheric Temperature Climate Data Record from Merged SSU and AMSU-A Observations, *Journal of Atmospheric and Oceanic Technology*, 33 (2016) 1967-1984.
45. D.J. Seidel, J. Li, C. Mears, I. Moradi, J. Nash, W.J. Randel, R. Saunders, D.W.J. Thompson, C.-Z. Zou, Stratospheric temperature changes during the satellite era, *Journal of Geophysical Research: Atmospheres*, 121 (2016) 664-681.

46. W.J. Randel, A.K. Smith, F. Wu, C.-Z. Zou, H. Qian, Stratospheric Temperature Trends over 1979–2015 Derived from Combined SSU, MLS, and SABER Satellite Observations, *Journal of Climate*, 29 (2016) 4843-4859.